

## Temporal Sampling Requirements for Automatic Rain Gauges

JEFFREY A. NYSTUEN

*Applied Physics Laboratory, University of Washington, Seattle, Washington*

(Manuscript received 27 November 1996, in final form 15 December 1997)

### ABSTRACT

Automatic rain gauges are needed to obtain rainfall statistics from remote locations and platforms. Many of these platforms cannot be serviced regularly, thus requiring unattended operations for many months. At such locations there is often a power consumption limitation requiring that the instrument operate at a fractional duty cycle. For instruments that measure rainfall rate rather than rainfall accumulation, both components of duty cycle—sample duration and sample interval—need to be considered. A 17-month-long record of rainfall was recorded in Miami, Florida. This location is subtropical and has an annual rainy season. These data are subsampled using different duty cycles to assess resulting sampling error. Using 1-min rainfall-rate samples, a duty cycle of 10% produces an expected standard deviation in monthly rainfall accumulation equal to 10% of the mean accumulation. This relationship held true for 15 of the 17 months of data. Two months with very low total accumulations (November 1993 and March 1994, both winter season months) had higher errors. For a fixed duty cycle, sampling error is proportional to both sampling duration and sample interval.

### 1. Introduction

Quantitative knowledge of the global water budget is of key importance to understanding the earth's climate system. In particular, the frequency and distribution of global rainfall is a climatic measurement that has been identified as crucial. Globally, most rainfall occurs in the tropical regions (see, e.g., Legates and Willmott 1990), and most of this rainfall occurs over the oceans or rain forests. These are difficult regions to sample rainfall, as relatively few people live in them. Thus, there is a need for rainfall measurements from remote platforms—ocean moorings, for example—that are unattended for months at a time. Attempts to provide global estimates of the distribution of oceanic rainfall have been made using qualitative ship weather reports (e.g., Tucker 1961; Legates and Willmott 1990; Petty 1995) and satellite data (e.g., Arkin and Xie 1994; Barrett et al. 1994). Significant discrepancies between these efforts exist, and extensive research into this topic is ongoing (Ebert et al. 1996). One of the biggest problems is the lack of adequate surface measurements of rainfall (Barrett et al. 1995).

Recently, several types of automatically recording rain gauges have been developed. Several of these show promise for deployment in remote locations, including ocean buoys. These systems include collection-type gauges (capacitance rain gauge); rainfall-rate gauges

(optical rain gauge); disdrometers, which measure individual drop impacts; and underwater acoustical systems, which measure rainfall rate and integrated drop distributions. At remote locations, power limitations may require fractional duty cycles. This is composed of two components: sample duration and sample interval, where sample duration is the time that the sensor is on and sample interval is the time between the start of each cycle. The sampling demands for collection-type gauges and rainfall-rate gauges are different. For collection-type gauges, the assumption that all rainfall between samples is collected allows the additional assumption that sample duration equals sample interval. This permits focus on sampling interval alone (e.g., Morrissey et al. 1994). For rainfall-rate-type gauges, both sampling duration and sample interval need to be considered.

Temporal and spatial sampling strategies have been the subject of many recent efforts to understand how radar and satellite rainfall measurement statistics can be combined with surface rain gauge networks to yield calibration and measurement of regional and global rainfall statistics (e.g., Laughlin 1981; North and Nakamoto 1989; Bell et al. 1990; Fabry et al. 1994). These studies have generally focused on the sampling requirements for entire rain gauge networks rather than on the sampling errors associated with varying duty cycles of individual rain gauges. One result applicable to the present study is that sampling error increases with sample interval, one component of duty cycle (Laughlin 1981; Fabry et al. 1994). Steiner (1996) specifically addresses sparse temporal sampling from rain gauges, although again concentrating on sample interval rather than on

---

*Corresponding author address:* Dr. Jeffrey A. Nystuen, Applied Physics Laboratory, University of Washington, 1013 NE 40th Street, Seattle, WA 98105-6698.

both components of duty cycle. Using 15-min-duration rain gauge data from Darwin, Australia, and Melbourne, Florida, Steiner predicts that a temporal duty cycle of roughly 10% would yield accumulation measurements within 10% of the true accumulation. He also predicts that this sampling error is proportional to the sampling interval and is dependent on total accumulation:

$$E = \alpha \Delta t R^{-0.6},$$

where  $E$  is the coefficient of variation,  $\Delta t$  is the sampling interval,  $R$  is the total accumulation (usually monthly), and  $\alpha$  is a constant for this study but contains components of the spatial characteristics of the rain gauge networks in other studies.

In order to analyze the issue of duty cycle for automatic rain gauges, data from the rain gauge facility at the Atlantic Oceanographic and Meteorological Laboratory (AOML) are examined. This facility includes the four types of automatic rain gauges previously mentioned (optical, capacitance, disdrometer, and acoustic) plus weighing and tipping-bucket rain gauges. Technical details and intercomparison of the different rain gauge systems within the AOML facility are found in Nystuen et al. (1996) and will be summarized only briefly here. The location, Virginia Key, Miami, Florida, has a subtropical climate for most of the year, and most precipitation falls as part of subtropical mesoscale convective systems (MCS) (Houze 1989). Thus, temporal sampling strategies for the AOML rain gauge facility may be applicable to other tropical locations.

The objective of this effort, to assess the temporal sampling requirements for automatic rain gauges, can be achieved using any of the rain gauges within the AOML rain gauge facility, provided that the rain gauge operated consistently throughout the experiment. The data from the entire deployment, 17 months of continuous rainfall data, including several different rainfall seasons, is examined. The most consistent rain gauge within the system is the R. M. Young capacitance gauge. Data from this gauge are further analyzed to address the temporal sampling issue.

## 2. Experimental setup

### a. The AOML rain gauge facility

The AOML rain gauge facility surrounds a brackish water pond adjacent to the AOML building on Virginia Key (25.7°N, 80.1°W). The rain gauges in the AOML rain gauge facility include 1) a weighing rain gauge; 2) an R. M. Young Model 50202 capacitance rain gauge; 3) several Scientific Technologies (ScTI) ORG-105 optical rain gauges; 4) a Belfort Model 382 tipping-bucket rain gauge; 5) two disdrometers: a Distromet RD-69 disdrometer and an Applied Physics Laboratory–John Hopkins University (APL–JHU) prototype; and 6) an acoustical rainfall system using an ITC-4123 hydrophone. An R. M. Young Model 05103 anemometer was

also part of the system. All rain gauges were within 50 m of each other. The capacitance, optical, and tipping-bucket rain gauges were within 5 m of each other.

### b. Technical description of the rain gauges

A more complete technical description of each rain gauge is found in Nystuen et al. (1996). A brief review is included here to give the reader a feel for the characteristics of the rain gauge instruments involved and the types of error that are to be expected for each gauge. In general, all of the rain gauges within the AOML facility worked well; however, each has its limitations. The most consistent rain gauge within the AOML facility, based on lack of outliers and reliability, was the R. M. Young capacitance rain gauge. Temporal analysis in section 3 uses the data from this gauge only.

#### 1) WEIGHING RAIN GAUGE

The weighing rain gauge operates on the principle of weighing the rainwater collected by the instrument. The measurement of rainfall rate is the difference in rainwater accumulation over a given time interval. The accuracy of the rainfall-rate measurement is controlled by the precision of the water accumulation measurement, the rate at which rainwater drains from the catchment basin into the measurement chamber, and the sampling interval. For a 1-min sampling interval, this instrument performs relatively well for rainfall rates over 5 mm h<sup>-1</sup>. As rainfall rate drops below 5 mm h<sup>-1</sup>, flow characteristics, the movement of water from the catchment basin into the measurement chamber, begin to cause instrument “noise” for short sampling intervals. This noise is reduced for longer sampling intervals. Technical difficulties with the automatic drainage system in the AOML instrument resulted in loss of data during several major events.

#### 2) R. M. YOUNG CAPACITANCE RAIN GAUGE

The capacitance rain gauge is a collection-type gauge that was developed for potential use on buoys at sea (Holmes et al. 1981; Holmes and Michelena 1983). A probe consisting of a stainless steel rod covered by a Teflon sheath is set inside a cylindrical collection chamber. The water surrounding this probe forms the outer “plate” of a coaxial-type capacitor, while the metal rod forms the inner “plate.” As the water height in the collection chamber rises, the surface area of the capacitor increases, increasing the capacitance. The capacitance is measured and converted to water height in the collection chamber. As with the weighing rain gauge, the measurement of rainfall rate is the difference in rainwater accumulation over a given time interval.

The capacitance rain gauge used in the AOML rain gauge facility is an R. M. Young Company Model 50202 precipitation gauge. This gauge performs well for rain-

fall rates over  $5 \text{ mm h}^{-1}$ . Again, as rainfall rate drops below  $5 \text{ mm h}^{-1}$ , flow characteristics of the instrument can cause errors in 1-min rainfall rates of up to  $+10 \text{ mm h}^{-1}$ ; however, this noise for rainfall rate is part of the true long-term accumulation. This gauge worked reliably throughout the experiment.

### 3) BELFORT TIPPING-BUCKET RAIN GAUGE

Tipping-bucket rain gauges measure rainfall by allowing rainwater to drain into a bucket that tips and drains after a given amount of rainwater has been collected. Each tip triggers a magnetic switch that sends a signal to a recording device. These instruments are widely used in automatically recording hydrographic arrays on land. The principal flaw for this instrument is the occasional failure to tip during an event. This is usually due to fouling, which is often biological in nature. At extremely high rainfall rates, this type of gauge will underestimate rainfall rate. This type of rain gauge is unsuitable for deployment at sea.

### 4) SCTI OPTICAL RAIN GAUGES

Optical rain gauges (ORG) measure the scintillation in an optical beam produced by the shadows of raindrops falling between a light source [a light-emitting diode (LED)] and an optical receiver (Wang and Clifford 1975; Wang et al. 1977; Wang et al. 1978). The light intensity variation due to the shadow of a given drop is a function of drop size, fall velocity, optical geometry, and coherence of the LED light source. By choosing the proper geometry, the intensity variation caused by natural raindrops is proportional to rainfall rate (Wang et al. 1978).

The AOML rain gauge facility uses ORG-105s, built by Scientific Technologies, Inc. The optical rain gauges have an instrument error when measuring 1-min rainfall rates of roughly  $\pm 20\%$ , which is independent of rainfall rate over  $1 \text{ mm h}^{-1}$ . A dependence on the drop size distribution of the particular rain being measured is suspected. These instruments also have a background noise, that is, electrical noise, usually equivalent to  $0.2\text{--}0.4 \text{ mm h}^{-1}$ . This noise is assumed to be additive to the real rain signal and has been "removed" from the data reported here by identifying the background noise level in the absence of rain and then subtracting the noise from the measurements during rain.

### 5) DISDROMETERS

A disdrometer is designed to measure the actual drop size distribution within rain by converting the momentum of individual raindrops striking the sensor head into an electronic signal proportional to drop size. The actual relationship depends on the characteristics of the sensor head. As each raindrop hits the sensor surface, the mo-

mentum of the impact is translated into an electrical pulse proportional to drop size.

Two types of disdrometer were used: the Joss–Waldvogel disdrometer (Joss and Waldvogel 1967, 1969) was in the system from 25 September 1993, and a prototype APL–JHU disdrometer (Roland 1976) was operational in October and November 1994, and January 1995. This type of gauge performs well for rainfall rates over  $5 \text{ mm h}^{-1}$ . As the rainfall rate decreases to under  $5 \text{ mm h}^{-1}$ , the sampling area begins to become too small to adequately sample the rainfall using a 1-min sampling interval. At extremely high rainfall rates, instrument duty cycle (processing time for each drop) results in underestimates of drop counts (Sheppard and Joe 1994), resulting in an underestimation of extremely heavy rainfall rates (over  $100 \text{ mm h}^{-1}$ ).

#### c. Description of the data

The AOML rain gauge facility was operational from September 1993 until the end of January 1995 (17 months). During this period, more than 800 rain events occurred. A rain event was defined as any precipitation period with a rainfall rate over  $1 \text{ mm h}^{-1}$  and lasting at least 5 min. The automatic trigger for recording an event was the signal from one of the optical rain gauges. Whenever this signal indicated at least  $1 \text{ mm h}^{-1}$  rainfall, the system turned on. The system automatically resumed "rest" mode 5 min after the signal from the optical rain gauge dropped below  $1 \text{ mm h}^{-1}$  (and stayed below  $1 \text{ mm h}^{-1}$ ). Thus, the minimum event length was 5 min. The data were subjectively examined to eliminate events with spurious or minimal triggers.

For each month, all rainfall events were combined into a single dataset. Each record consists of the minute during the month and the 1-min-average rainfall rate from each rain gauge for that minute. Figure 1 shows the accumulation totals for each rain gauge as a function of month. There is general agreement among gauges. In fact, using more than 9000 1-min rainfall-rate data points, the interinstrument correlation coefficients are of order 0.95.

#### d. Choosing the "best" rain gauge

Selecting the "best" rain gauge for further analysis is subjective. All rain gauges have known flaws, and, even if they operate perfectly, rainfall is not spatially homogeneous. So the "true" rainfall at the AOML site is unknown. There are several choices for any given time period. The gauge that appeared to operate the most consistently throughout the experiment was the capacitance rain gauge. In fact, the disdrometer is likely to be closer to the truth in September 1994, as the rest of the gauges missed a couple of large accumulation events. However, the disdrometer data from May until June 1994 is incomplete because it was physically removed from the field for calibration and evaluation. The

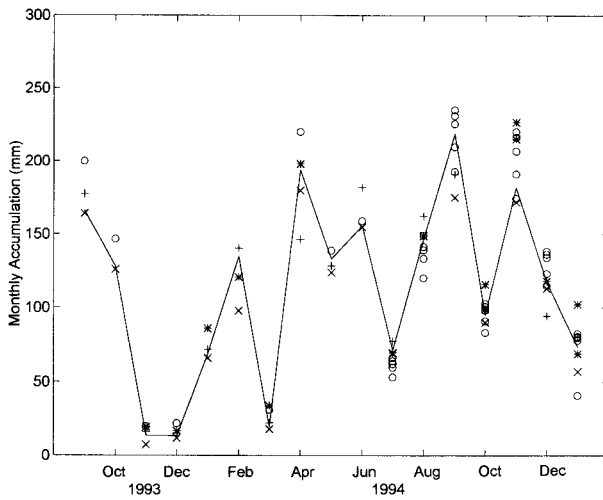


FIG. 1. Monthly rainfall accumulation summary. Data from the capacitance (solid line), optical (circle), tipping-bucket ( $\times$ ), weighing (+), and disdrometer (\*) rain gauges are shown. During several large accumulation events, one or more of the gauges failed (weighing, tipping bucket) or were physically removed from the field (disdrometers), resulting in monthly accumulation outliers. These data points are not shown.

optical rain gauges showed a seasonal variability, biasing high during months of relatively light mean rainfall rates. Furthermore, several different optical instruments were deployed. The tipping bucket is known to have failed during several events because of biological fouling. Also, 1-min rainfall-rate data from the tipping-bucket rain gauge is particularly noisy ( $\pm 12 \text{ mm h}^{-1}$ ). Throughout the experiment, the capacitance gauge performed consistently and was never an outlier for monthly accumulation. It did “fail” during several minor events in January 1994. However, it is chosen as the best rain gauge for further analysis.

One interesting calculation is to estimate the error associated with choosing a particular rain gauge as the best one. Using Fig. 1, accumulation totals are available for each month from each rain gauge. The statistic “coefficient of variation” (Cramer 1945), the standard deviation divided by the mean, can be used to describe the likelihood that a measurement will be within a given percentage of the true accumulation. For example, given a normal positive distribution of accumulation measurements, a coefficient of variation of 0.1 implies that a measurement will be within 10% of the true accumulation 68% of the time, and so on. The coefficient of variation associated with instrument choice as a function of month is shown in Fig. 2. The value for most months is around 0.1. Thus, the choice of instruments accounts for 10% of the scatter about the sample mean accumulation. This shows the difficulty of making rainfall measurements. Either there is an inherent spatial scale of rainfall variation at the Miami site or there are interinstrument biases—imperfect calibrations, for example—present, although each instrument was cali-

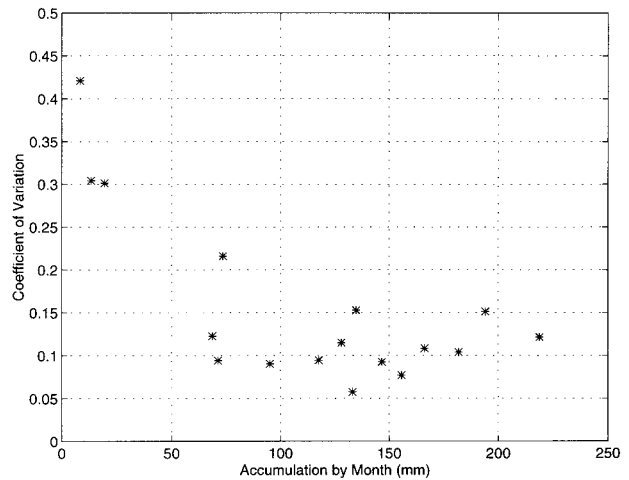


FIG. 2. Coefficient of variation of rainfall accumulation due to choice of rain gauge. The different rain gauges allow a mean and standard deviation of rainfall accumulation to be calculated for each month.

brated. Of course, if interinstrument biases can be documented and corrected for, then these errors will be reduced. By choosing one instrument to be “correct,” temporal sampling strategies can be explored without considering these interinstrument biases further.

### 3. Data analysis

#### a. Virginia Key climatology

One of the most important factors to recognize when choosing a temporal sampling strategy for rainfall is the local climatology. Temporal sampling requirements for long-duration, light rainfall are very different than for short, intense rainfall. Technically, the results of this study are applicable to Virginia Key for the 17 months of the experiment. However, by describing the rainfall encountered at Virginia Key during this experiment, transferability of the conclusions to other locations is possible.

Virginia Key is located at  $25.7^{\circ}\text{N}$ ,  $80.1^{\circ}\text{W}$ , several miles off the southeastern Florida coast at Miami. The climate is subtropical most of the year. The region is occasionally affected by tropical storms, one of which was Tropical Storm Gordon in November 1994. Figure 3 shows the mean rainfall rate and wind during rain as a function of month during this experiment. Three distinctive regimes are detected. During the winter months, the mean rainfall rates tended to be light,  $2 \text{ mm h}^{-1}$ , with mostly southerly winds. This was due to relatively weak convective systems and a few long-duration, light rainfall-rate events associated with the continental mid-latitude frontal systems. During the rainy season (August–October), mean rainfall rates are higher ( $4\text{--}7 \text{ mm h}^{-1}$ ), as the convective systems are usually stronger. The winds were generally from the northeast ( $50^{\circ}$ ). During the spring transition months (April–June), several very

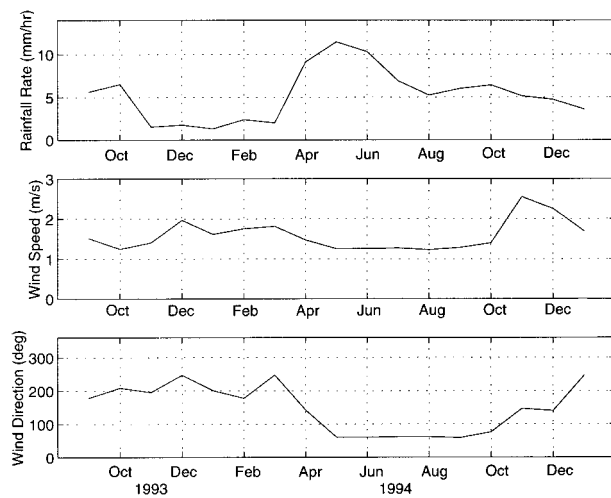


FIG. 3. A summary of mean conditions at the AOML site (Virginia Key, FL). Top: mean rainfall rate during rain. Middle: mean wind speed during rain. Bottom: mean wind direction during rain. Three seasons are suggested: winter (November–March) with low mean rainfall rates and winds from the south, spring (April–June) with high mean rainfall rates from intense convective systems, and the rainy season (July–October) with moderate mean rainfall rates and winds from the east. Tropical Storm Gordon occurred in November 1994 with relatively high winds.

intense rainfall events occurred, resulting in a high mean rainfall rate (more than  $10 \text{ mm h}^{-1}$ ). The temporal character of the rain from these different periods is shown in Fig. 4. Gaps between rain events have been removed to allow 500 min of rainfall data to be shown for each time period. (Subsequent analyses use the original data, including nonraining times.) The September 1993 data show the character of the rainy season convective events, which are mostly short duration with a temporal scale of fewer than 5 min (autocorrelation time). The long-duration, lighter rainfall-rate data from a “winter” system are shown in the February 1994 record (note: different rainfall-rate scale). The temporal scale is longer, on the order of 10 min. The temporal scale of May 1994 is also of order 10 min due to the longer-duration, intense rainfall events recorded then. Finally, the temporal record of Tropical Storm Gordon in November 1994 shows the short, spiky nature of the events associated with this storm. Tropical Storm Gordon also had relatively high mean winds (Fig. 3). Otherwise, mean wind speeds at the Virginia Key site were relatively low, less than  $2 \text{ m s}^{-1}$ . High wind speeds are a known source of instrument error for accumulation-type rain gauges (e.g., Legates and deLiberty 1993) and thus the low winds at the Virginia Key site are ideal for intercomparison studies of rain gauges. In the rainy season (August–October), there was a weak diurnal cycle to the rain showing an evening rainfall minimum from 1800 to 2400 LT and a weak maximum from 0500 to 1000 LT. Otherwise, the rainfall at Virginia Key did not show any diurnal patterns.

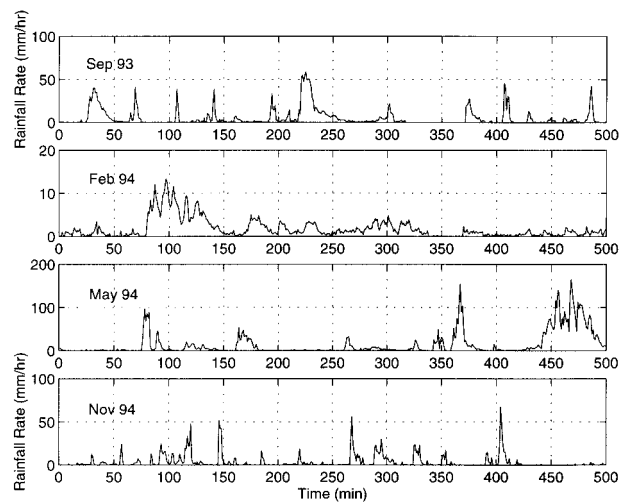


FIG. 4. Time series of rainfall rate during four different seasons. The September 1993 time series shows the character of mostly moderate rainy season convective systems with an autocorrelation time of roughly 5 min. The February 1994 record shows the character of a longer, sustained light rain occurring during the winter season with an autocorrelation time of roughly 10 min. May 1994 shows an intense event, with a decorrelation time of 10 min, and November 1994 shows the short, spiky character of the rainfall during Tropical Storm Gordon. The decorrelation timescale for Tropical Storm Gordon is roughly 4 min.

#### b. Temporal sampling analysis

For each month, the 1-min rainfall rate for each minute is specifically identified. These data are then subsampled using several different regular sampling intervals, simulating a duty cycle for an automatic rain gauge. The rainfall rate within a given sampling interval is assumed to be constant over that entire sampling interval. If every other minute is sampled (2-min sampling interval), then two estimates of the total rainfall accumulation for that month are available. Similarly, 5 estimates are available for the 5-min sampling interval, 10 for 10 min, and so on (Fig. 5). As the sampling interval becomes long, the distribution of accumulation totals is not normally distributed but rather skewed. This is because of the very short duration, extremely high rainfall rates associated with the convective cells. If the duty cycle is too low, then short-duration, extremely high rainfall rate events will be missed too often to adequately sample the total accumulation. The coefficient of variation requires only a positive distribution (Cramer 1945), so it can be calculated for each sampling interval. The rate of increase of the coefficient of variation as a function of sampling interval (the slope of the dashed lines in Fig. 5) shows the linear trend as predicted by Steiner (1996).

Figure 6 shows the coefficient of variation as a function of monthly accumulation for a 10% duty cycle using 1-min duration samples. The value is near 0.1 for 15 of the 17 months. During two low-accumulation months (November 1993 and March 1994), the error is higher.

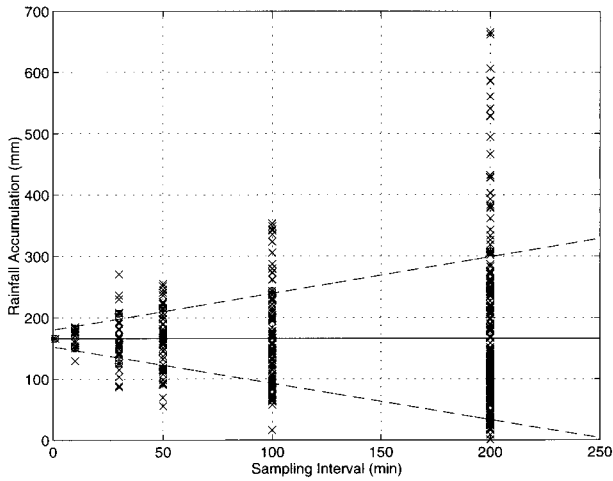


FIG. 5. Estimated rainfall accumulations using different sampling intervals on the September 1993 capacitance rain gauge data. The sample duration is 1 min. The rainfall rate is assumed to be constant for the entire sampling interval. Multiple estimates of monthly accumulation are available for sampling interval longer than 1 min; for example, 10 estimates are possible using a 10-min sampling interval. The solid line shows the accumulation using all of the data, the truth. For each sampling interval, the coefficient of variation, the standard deviation divided by the mean accumulation, can be calculated. The dashed line is the linear least squares fit to the mean  $\pm$  standard deviation ( $\oplus$  symbol) at each sampling interval.

A high coefficient of variation when the total accumulation is low is not a large accumulation error. This is merely an indication that in situations in which relatively little rainfall occurs (in a few isolated events), temporal sampling demands are higher. Also, as the mean approaches zero, the utility of coefficient of variation (standard deviation divided by mean) is reduced. Note that for monthly accumulations above 50 mm, there is little suggestion of a dependence on total accumulation.

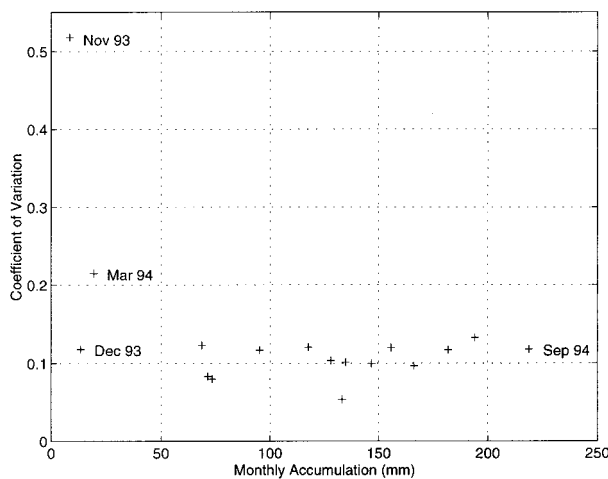


FIG. 6. Coefficient of variation for each month using a 10% duty cycle of 1-min-duration samples every 10 min.

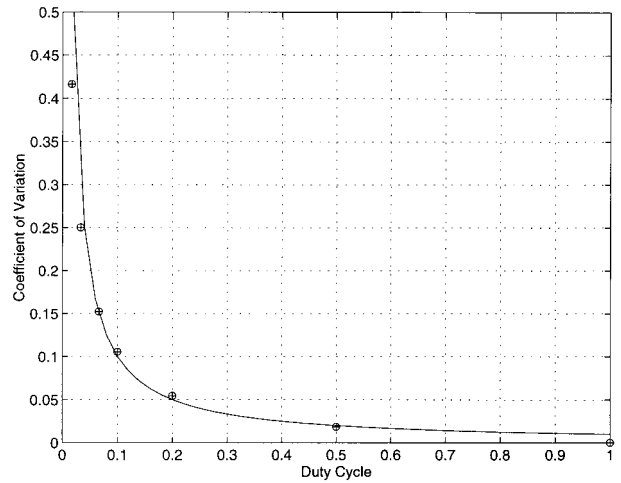


FIG. 7. The coefficient of variation as a function of duty cycle using 1-min-duration samples. The solid line shows  $E = 0.01/dc$ , where  $dc$  is duty cycle. Two months (November 1993 and March 1994) are not included.

Figure 7 shows the coefficient of variation as a function of duty cycle, with the two low-accumulation months (November 1993 and March 1994) removed. It is approximately inversely proportional to the duty cycle—although as duty cycle approaches unity and sampling error goes to zero, this relationship must break down. This is because of the finite duration for a single sample.

The influence of the single-sample duration on the coefficient of variation is shown in Fig. 8. Given a fixed duty cycle, as the sample duration increases, the temporal gap between measurements increases. For example, using the sampling strategy of Steiner (1996), a measurement duration of 15 min, a 10% duty cycle implies a gap of 135 min (more than 2 h) between mea-

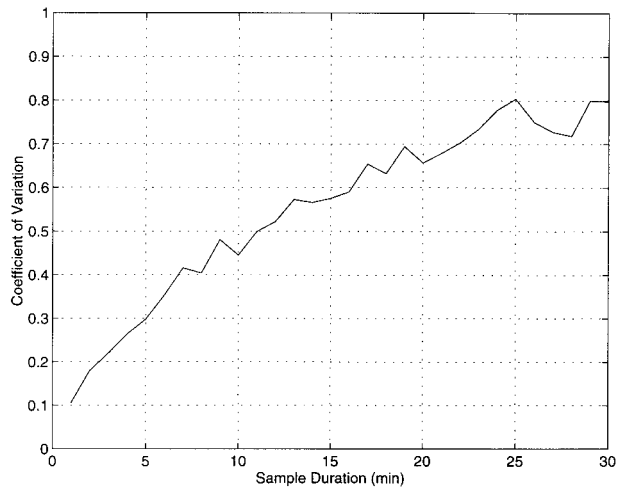


FIG. 8. The coefficient of variation as a function of sample duration for a duty cycle of 10%. Two months (November 1993 and March 1994) are not included.

surements, whereas the gap between measurements using a 1-min sample is only 9 min. Increasing the sample duration from 1 to 15 min increases the coefficient of variation from 0.1 to roughly 0.4. The average duration of rain events in the Virginia Key dataset is 26 min. Thus, a sample every 10 min will “sample” most rain events; however, a sample every 2.5 h will miss many events, leading to a higher probability of error.

### c. Discussion

If the goal of a temporal sampling strategy is to achieve a given coefficient of variation—for example, 0.1—then several factors need to be considered. These include the duty cycle of the instrument and its components, the sampling interval, and the sample duration. Given Fig. 7, the “optimal” duty cycle using a 1-min measurement is about 10%. The reduction in the coefficient of variation as the duty cycle goes from 20% to 100% is relatively small. On the other hand, as the duty cycle drops below 10%, the coefficient of variation increases rapidly. This suggests an optimal sampling duty cycle of about 10%. Of course, if one can afford a higher duty cycle, the sampling error can be reduced. For rainfall accumulation instruments—for example, the capacitance gauge—this is achieved by assuming that all of the rainfall collected between samples is accumulated. However, for the rainfall-rate instruments—for example, optical, disdrometer, or acoustic gauges—increasing the sample duration will have a power consumption cost.

Steiner (1996) suggests that on 8.3% duty cycle (15-min sample every 3 h) will achieve a coefficient of variation of 0.1. Although it seems to be in apparent agreement with these data, in fact, it is not. A 10% duty cycle with 15-min samples produces a coefficient of variation of roughly 0.6 (Fig. 8). Apparently, the rainfall at Darwin and at Melbourne is fundamentally different than the Virginia Key data. At both Darwin and Melbourne, significant diurnal patterns in the rainfall are present (Steiner 1996). Furthermore, monthly rainfall accumulations are higher. These two features of the rain apparently reduce the sampling requirements for these locations. Steiner also reports a dependence on total accumulation. This is not apparent in these data for accumulations over 50 mm, at least for 1-min rainfall samples at 10% duty cycle (Fig. 6). The dependence of the coefficient of variation on total accumulation probably depends on the likelihood of adequately sampling for each event. Regardless of duty cycle, if the interval between samples is frequent enough to sample each event, then the sampling error will be reduced. On the other hand, if this interval is longer than a typical event, the sampling error will be higher. The average duration of a rain event in the Miami data is 26 min, so sampling for 1 min every 10 min will detect most events, whereas a 10-min sample every 100 min will miss many events. Once events are adequately sampled—that is, several

measurements for each event—these data suggest that the coefficient of variation is independent of total accumulation.

## 4. Conclusions

Rainfall data collected during 17 months at Virginia Key are examined to determine an appropriate duty cycle for automatically recording rain gauges. The data are smoothed to 1-min rainfall-rate data for each of several automatic rain gauge systems. These data are subsampled at different duty cycles. The monthly rainfall accumulation totals are estimated for each duty cycle, and the coefficient of variation (the standard deviation divided by the mean) is calculated for each month. The duty cycle of 10% using 1-min duration measurements, that is, a 1-min sample every 10 min, produces a coefficient of variation equal to 0.1. In fact, this measure of error depends on duty cycle and both of its components: sampling interval and sample duration. The same 10% duty cycle using 15-min-duration rainfall samples produces a coefficient of variation equal to 0.6. The error is inversely proportional to duty cycle. For a fixed duty cycle, the error is proportional to both sample duration and sample interval. In an operational system, additional errors associated with instrument accuracy and spatial variation in rainfall will also be present.

*Acknowledgments.* The AOML rain gauge facility was developed through the efforts of John Proni, Peter Black, and John Wilkerson. Engineering support for the facility was provided by J. Bufkin, U. Rivero, C. Lauter, M. Boland, and J. Stamates. Comments from M. Steiner and the referees are appreciated. Financial support for data analysis is from NSF and NOAA/NDBC.

## REFERENCES

- Arkin, P. A., and P. Xie, 1994: The Global Precipitation Climatology Project: First Algorithm Intercomparison Project. *Bull. Amer. Meteor. Soc.*, **75**, 401–419.
- Barrett, E. C., J. Dodge, M. Goodman, J. Janowiak, and E. Smith, 1994: The First WetNet Intercomparison Project (PIP-1). *Remote Sens. Rev.*, **11**, 49–60.
- , C. Kidd, and D. Kniveton, 1995: The First WetNet Precipitation Intercomparison Project (PIP-1): Reflections on the results. *Proc. IGARSS '95*, Florence, Italy, IEEE Geoscience and Remote Sensing Society, 649–651.
- Bell, T. L., Abdullah, R. L. Martin, and G. R. North, 1990: Sampling errors for satellite-derived tropical rainfall: Monte Carlo study using a space–time stochastic model. *J. Geophys. Res.*, **95**, 2195–2205.
- Cramer, H., 1945: *Mathematical Methods of Statistics*. Princeton University Press, 575 pp.
- Ebert, E. E., M. J. Manton, P. A. Arkin, R. J. Allam, G. E. Holpin, and A. Gruber, 1996: Results from the GPCP Algorithm Intercomparison Programme. *Bull. Amer. Meteor. Soc.*, **77**, 2875–2887.
- Fabry, F., A. Bellon, M. R. Duncan, and G. L. Austin, 1994: High-resolution rainfall measurements by radar for very small basins: The sampling problem reexamined. *J. Hydrol.*, **161**, 415–428.

- Holmes, J., and E. Michelena, 1983: Design and testing of a new rain gauge for NDBC meteorological data buoys. Preprints, *Fifth Symp. Meteorological Observations and Instrumentation*, Toronto, ON, Canada, Amer. Meteor. Soc., 34–37.
- , B. Case, and E. Michelena, 1981: Rain gauge for NOAA data buoys. *Proc. IEEE/MTS Symp. Oceans '81*, Boston, MA, IEEE Council on Oceanic Engineering and Marine Technical Society, 463–467.
- Houze, R. A., Jr., 1989: Observed structure of mesoscale convective systems and implications for large-scale heating. *Quart. J. Roy. Meteor. Soc.*, **115**, 425–461.
- Joss, J., and A. Waldvogel, 1967: Ein Spektrograph für Niederschlags-tropfen mit automatischer Auswertung. *Pure Appl. Geophys.*, **68**, 240–246.
- , and —, 1969: Raindrop size distribution and sampling size errors. *J. Atmos. Sci.*, **26**, 566–569.
- Laughlin, C. R., 1981: On the effect of temporal sampling on the observation of mean rainfall. Precipitation Measurements from Space Workshop Report, 358 pp. [Available from NASA/Goddard Space Flight Center, Greenbelt, MD 20771.]
- Legates, D. R., and C. J. Willmott, 1990: Mean seasonal and spatial variability in gauge-corrected global precipitation. *Int. J. Climatol.*, **10**, 111–127.
- , and T. L. deLiberty, 1993: Precipitation measurement biases in the United States. *Water Resour. Bull.*, **29**, 855–861.
- Morrissey, M. L., W. F. Krajewski, and M. J. McPhaden, 1994: Estimating rainfall in the tropics using fractional time raining. *J. Appl. Meteor.*, **33**, 387–393.
- North, G. R., and S. Nakamoto, 1989: Formalism for comparing rain estimation designs. *J. Atmos. Oceanic Technol.*, **6**, 985–992.
- Nystuen, J. A., J. R. Proni, P. G. Black, and J. C. Wilkerson, 1996: A comparison of automatic rain gauges. *J. Atmos. Oceanic Technol.*, **13**, 62–73.
- Petty, G. W., 1995: Frequencies and characteristics of global oceanic precipitation from shipboard present-weather reports. *Bull. Amer. Meteor. Soc.*, **76**, 1593–1616.
- Roland, J. R., 1976: A comparison of two different raindrop disdrometers. Preprints, *17th Conf. on Radar Meteorology*, Seattle, WA, Amer. Meteor. Soc., 398–405.
- Sheppard, B. E., and P. I. Joe, 1994: Comparison of raindrop size distribution measurements by a Joss–Waldvogel disdrometer, a PMS 2DG spectrometer, and a POSS Doppler radar. *J. Atmos. Oceanic Technol.*, **11**, 874–887.
- Steiner, M. A., 1996: Uncertainty of estimates of monthly areal rainfall for temporally sparse remote observations. *Water Resour. Res.*, **32**, 373–388.
- Tucker, G. B., 1961: Precipitation over the North Atlantic Ocean. *Quart. J. Roy. Meteor. Soc.*, **87**, 147–158.
- Wang, T. I., and S. F. Clifford, 1975: Use of rainfall-induced optical scintillations to measure path-averaged rain parameters. *J. Opt. Soc. Amer.*, **65**, 927–937.
- , G. Lerfald, R. S. Lawrence, and S. F. Clifford, 1977: Measurement of rain parameters by optical scintillation. *Appl. Opt.*, **16**, 2236–2241.
- , K. B. Earnshaw, and R. S. Lawrence, 1978: Simplified optical path-averaged rain gauge. *Appl. Opt.*, **17**, 384–390.